A COMPARISON OF THE SID-IIS ATD TO THE GLOBAL HUMAN BODY MODEL CONSORTIUM FIFTH PERCENTILE FEMALE MODEL IN THE INSURANCE INSTITUTE FOR HIGHWAY SAFETY (IIHS) UPDATED SIDE IMPACT CRASH TEST (SIDE 2.0).

Anthony Dellicolli
Jeff Dix
Nissan Technical Center North America
United States of America

Russ Morris
Benjamin K. Shurtz
Autoliv
United States of America

Paper Number 23-0282

ABSTRACT

This paper will present a study comparing the response of the SID-IIs Anthropomorphic Test Device (ATD) to the Global Human Body Model Consortium fifth percentile female model (GHBMC F05 v5.1) in the Insurance Institute for Highway Safety (IIHS) updated side impact crash test (Side 2.0). The study was conducted using a CAE model correlated to a barrier crash test with a small SUV. The occupant kinematics as well as injury response of the SID-IIs was compared to that of the Human Body Model (HBM). The SID-IIs response generally agreed well with the human body model except for clockwise pelvis Z-axis rotation resulting from the 'M-shaped' door deformation pattern characteristic of the IIHS Side Impact 2.0 test; additionally, the femur moment measured on the SID-IIs was significantly higher than that measured in the HBM. A CAE model of a simplified bending test was created to study the loading mechanism driving the femur moment responses and clarify the reasons for the differences observed for the HBM and SID-IIs. Through this study it was found that the SID-IIs hip allows for only 10-12 degrees plan view articulation before mechanical joint lockout occurs. In the barrier test the clockwise pelvis rotation of the SID-IIs resulted in the lockout of the hip joint on the SID-IIs. As a result, the femur moment unrealistically increased exponentially compared to that of the HBM after hip joint lockout occurred. As such the SID-IIs as currently designed does not provide a biofidelic response for femur moments and pelvis rotation in the IIHS Side Impact 2.0 test.

BACKGROUND

Introduced and implemented in 2003, the Insurance Institute for Highway Safety (IIHS) Side Impact Crashworthiness Evaluation Program started rating vehicles based upon three areas of performance in a single-moving, 90-degree, deformable barrier impact [1]. The three areas of performance were evaluating Anthropomorphic Test Device (ATD) injury metrics using a Side Impact Dummy (SID-IIs) representing a 5th percentile female in the front and rear seating positions, head protection, and vehicle structural performance. The SID-IIs was positioned in both the driver's position as well as the 2nd row left seating position during the test, and the 1,500kg (3,300lbf) moving deformable barrier (MDB) impacted the left side of the tested vehicle at 50kph (31mph). From this point forward in this paper, this original testing procedure will be referred to as IIHS Side Impact 1.0.

IIHS continued its side impact research, which included analysis of data from the National Automotive Sampling System (NASS), the Fatality Analysis Reporting System (FARS), and the Crash Injury Research and Engineering Network (CIREN), as well as full-scale vehicle-to-vehicle side impact tests and simulations [2, 3]. Through this research IIHS observed that despite vehicle performance improvements driven by their current side impact evaluations, serious injuries and fatalities were still occurring in currently "Good" rated vehicles. IIHS further identified that side impacts occurring in the field were resulting in greater intrusion, as well as more specific intrusion patterns, in the struck vehicle, and more specific occupant injuries.

IIHS desired to better represent the high severity side impact crashes observed through their field research [4, 5]. Analysis of internal vehicle-to-vehicle side impact testing showed a more specific type of deformation to the impacted vehicle, a deformation pattern that IIHS referred to as an 'M-shaped' deformation pattern [6, 7]. This deformation pattern, IIHS observed, had specific relationships to lower body loading. This led to the introduction of what is now commonly referred to as IIHS Side Impact 2.0, and changes to the program include an MDB redesign, increased impact speed, modifications to the ATD injury criteria, and changes to the overall rating scoring methodology [7]. To achieve the deformation pattern, the MDB honeycomb structure was redesigned, both in sub-component geometry and overall size, with the intent to better represent modern SUVs and Pickup Trucks. Further, the MDB cart also increased in mass to 1,900kg (4,189lbf), and the impact speed was increased to 60kph (37mph). Raising both the mass and speed resulted in an over 80% increase to the initial kinetic energy of the test between IIHS Side Impact 1.0 and 2.0 tests.

IIHS made modifications to the way they analyze ATD injury metrics, which included eliminating some of the measured injury parameters [8]. The eliminated parameters related to the pelvis and femur and included the individual iliac and acetabulum pelvic forces as well as the anterior-posterior and lateral-medial forces and moments at the femur. A summary of the common injury parameters between IIHS Side Impact 1.0 and 2.0 test, and their associated injury protection ratings, can be found in Table A within the Appendix.

While ATD's have been shown to demonstrate good correlation to human injury metrics for specific crash modes, environments, and locations on the human body, they are not without limitations [9, 10, 11]. Despite ongoing and well-researched improvements to ATD's in the last several decades, there are still areas of the human body where the use of man-made components as surrogates for biological tissues falls short of ideal representation [12, 13]. Human joints, specifically those with complex and multiple degrees of freedom, are challenging to re-create with mechanical components. The femur-pelvis interface is one of these complex joints.

An integral part of the worldwide effort to develop better tools for analyzing injury mechanisms and tolerances of human joints, as well as the entire human body, has been the Global Human Body Models Consortium (GHBMC). Created in 2006, the GHBMC strives to consolidate worldwide research and development activities to develop and maintain high-fidelity finite element human body models for automotive crash simulations. The consortium has established specific Centers of Expertise (COE) and Body Region Model (BRM) responsibilities within the overall global effort, including the body region comprising the pelvis and lower extremities. The research and development activities of the GHBMC include the purposeful collection of full-body 3D scanning data from live subjects, as well as the analysis of data collected during full-scale impact testing using human cadavers. An ongoing result of this work has been the development of continuously refined and improved models of a variety of sized and aged humans, including a fifth-percentile female model.

The objective of this paper is to compare the response of the SID-IIs and HBM in the IIHS Side Impact 2.0 test. To study this, injury response and kinematic comparisons are presented first between the SID-IIs in a IIHS Side Impact 2.0 physical vehicle test versus a representative CAE model and then later between the SID-IIs and the HBM in the same CAE model. In cases where the occupant behavior was not similar, further investigation was done to understand the reason for the difference.

METHODS

This study compared the occupant kinematics and injury response of the SID-IIs versus the HBM in the IIHS Side Impact 2.0 test using CAE modeling. The baseline physical data to correlate the model was a crash test of a small SUV in the IIHS Side Impact 2.0 test conducted according to the IIHS Crash Test Protocol (DRAFT - Version I, April 2020). Vehicle and driver ATD response data were collected and used as a reference for CAE model correlation.

ATD and HBM Information

All CAE simulations were conducted using LsDyna version mpp971_s_R9.3.1_140922. The SID-IIs model used in the simulations was version 4.3.2 from Humanetics, which was the latest version at the beginning of the study. This model represents the physical ATD used in the IIHS Side Impact 2.0 test. The HBM used in the study was the GHBMC 5th percentile female detailed model (GHBM F05-O v5.1). The 5th percentile HBM was selected as it represents the same size of occupant the SID-IIs was designed to represent.

Vehicle Test CAE Model

A vehicle test CAE model, including vehicle parts relevant to the driver interaction in the IIHS Side Impact 2.0 test, was created and designed to replicate the dynamic door deformation and seat pulse as input to the driver. The pulse inputs, as well as door trim and seat material characteristics and frictions were tuned until the SID-IIs kinematics and injury responses correlated to those of the SID-IIs in the physical vehicle test. The SID-IIs was then replaced in the CAE model with the HBM, and occupant kinematics and injury responses were compared. The simulation matrix is shown visually in Figure 1.

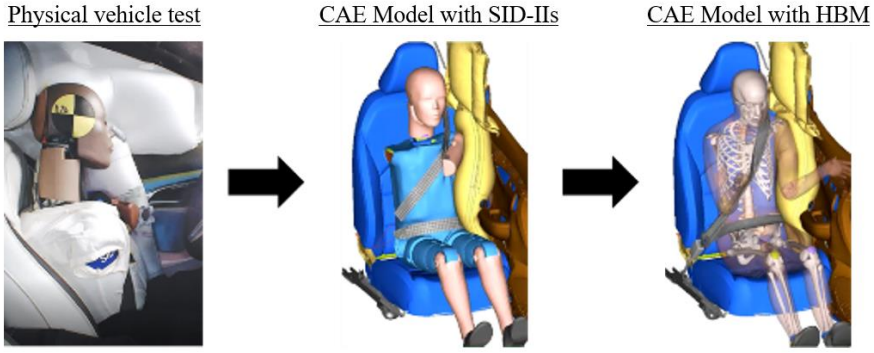

Figure 1. Simulation matrix: A CAE model with SID-IIs, correlated to a physical vehicle test, and then a CAE model that replaces the SID-IIs with the HBM.

The plan view of the post-test measurement laser scan section cut at the occupant H-point height of the physical test vehicle to which the CAE model is correlated exhibited the 'M-shaped' deformation pattern along the doors and B-pillar (See Figure 2). As previously mentioned, this deformation pattern is created by the design changes to the MDB honeycomb structure for the IIHS Side Impact 2.0 test.

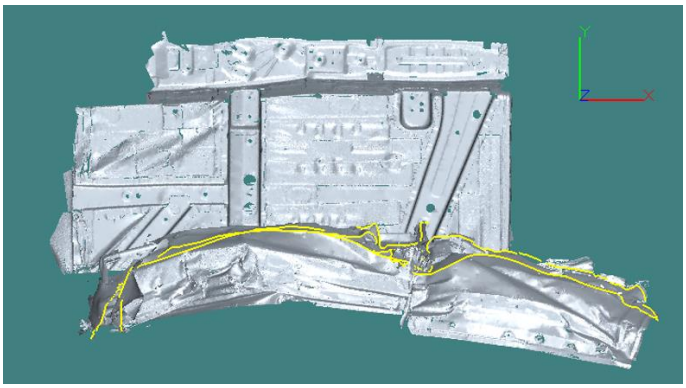

Figure 2. Plan view of the post-test measurement laser scan section cut at the occupant H-point height of the physical test vehicle.

Vehicle Test CAE Model Correlation

The CAE model with the SID-IIs dummy was developed to match the kinematics and injury responses of the physical IIHS Side Impact 2.0 vehicle test. The correlation of injury responses in the CAE model compared to the physical vehicle test can be seen in Figure 3.

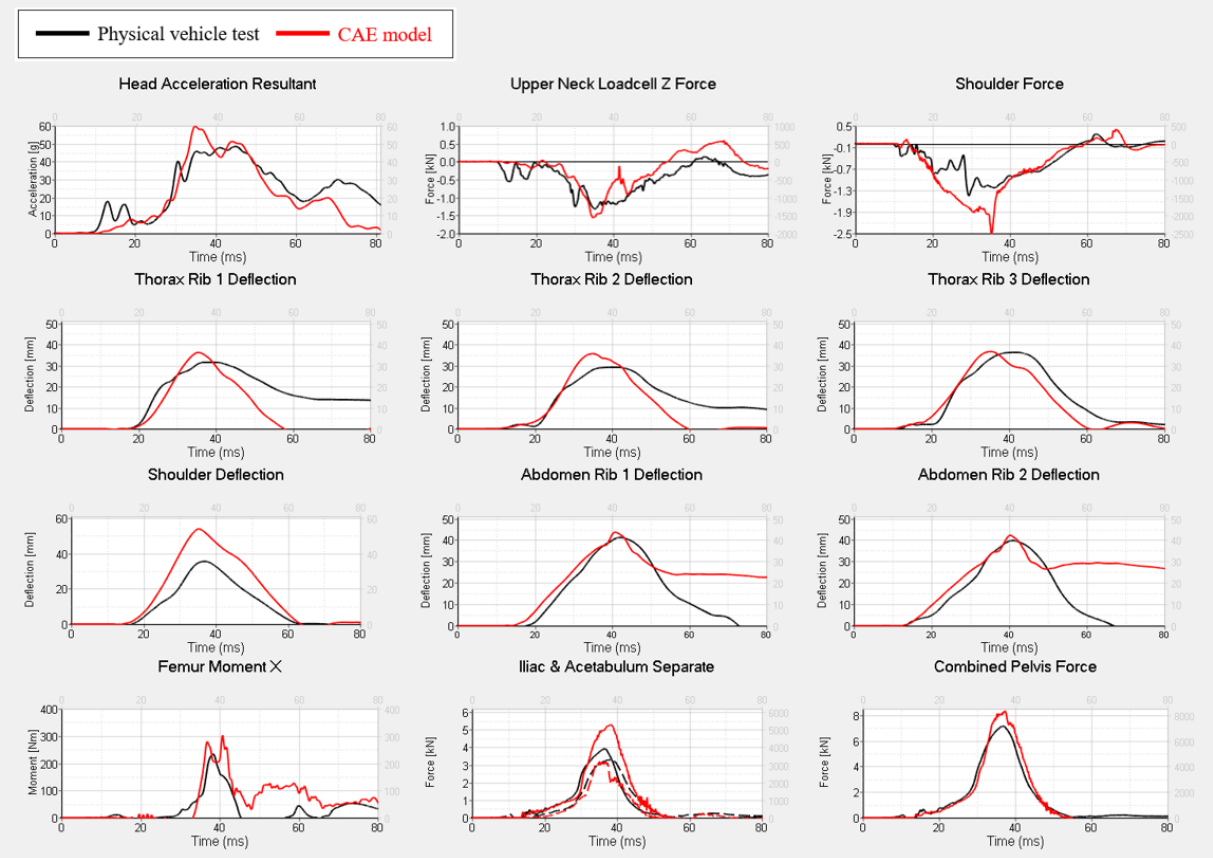

Figure 3. Injury response comparison between physical vehicle test and CAE model.

HBM Positioning

The positioning of the HBM (See Figure 4) was done in Primer v17.0. It was started by matching the H-point to that of the SID-IIs. The heel points were aligned to set the thigh and leg. The torso angle was matched. Then, the elbows were aligned to set the arm. Finally, the head center-of-gravity was matched.

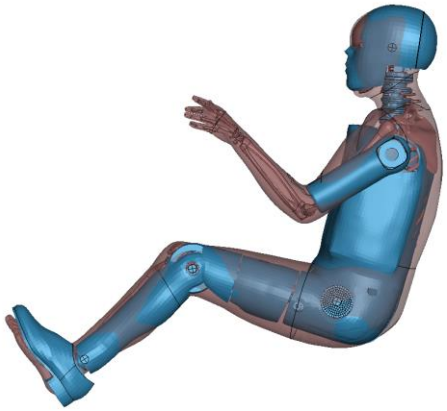

Figure 4. Overlay of the SID-IIs (blue) and HBM (brown) in their seated position for the CAE simulation.

Response Outputs

The CAE model of the SID-IIs comes from the supplier with instrumentation defined to measure accelerations, internal forces and moments, and local deflections of ribs at the same locations and using the same local coordinate systems as the physical dummy. For CAE correlation to the physical vehicle test, the responses of concern were those of the head, neck, shoulder, thorax, pelvis, and femur.

The F05-O HBM CAE model also comes from the supplier with pre-defined instrumentation to measure local accelerations of various body regions, internal forces and moments, and local deflections. In addition, the HBM can be used to predict bone fracture and internal organ injury based on the stresses and strains that develop during crash-induced loading. Because there is no rigid structure at the head CG, the head acceleration was output from a node located at the head CG that is constrained to a rigid skull plate using Ls-Dyna's constrained interpolation. The neck forces and moments were extracted from a cross-section through the C2 vertebra. For shoulder force, the HBM acromio-clavicle force measurement was selected as the nearest representation of the shoulder force an ATD would measure. For rib deflection measurement, the HBM model comes equipped with three virtual chestbands (See Figure 5).

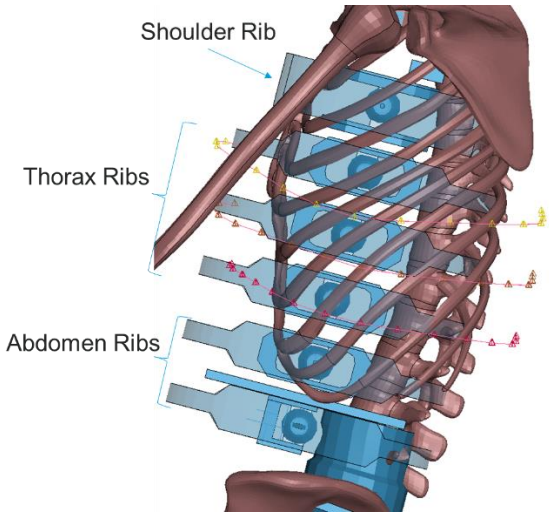

Figure 5. Chestbands on the HBM, located to align with the SID-IIs thorax ribs.

Thorax deflection was calculated from these chestbands using the half thorax deflection method, as is commonly done in physical side impact testing of post-mortem human surrogates [15, 16]. The left iliac and acetabulum forces along with the left femur X-axis moment were also output for comparison to the SID-IIs. The femur loadcell location in the F05-O v5.1 HBM pre-defined instrumentation was positioned more distal on the femur than the

loadcell in the SID-IIs. To ensure a fair comparison of HBM and ATD femur moments, an alternate femur loadcell was defined corresponding to the SID-IIs instrumentation (See Figure 6).

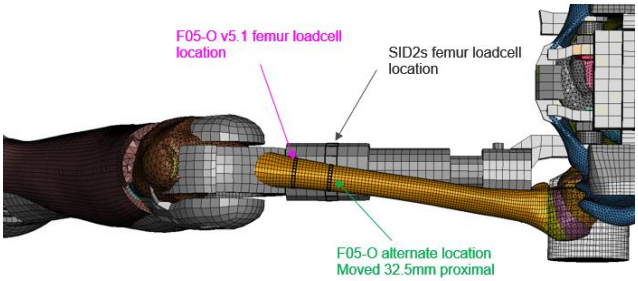

Figure 6. SID-IIs and GHBMC F05-O v5.1 femur loadcell definitions.

Simplified Femur Bending Test CAE Model

When the simulated SID-IIs and HBM results were compared, a large difference was seen in the measured femur x-moments of the two occupants. To better understand the femur moment and its relationship with thigh-pelvis Z-axis rotation, a CAE model of a simplified femur bending test was created and used to further compare response of the SID-IIs and HBM. The simplified model is shown in Figure 7 for the SID-IIs load case. A force was applied to the medial aspect of the knee to push the knee laterally. A constraint was also placed on the lateral aspect of the upper thigh to prevent lateral motion at that point. The locations of the forces correspond to one knee contacting the other while the thigh is constrained against the intruding door. The force couple in the bending simulation induced Z-axis rotation of the thigh (counterclockwise) relative to the pelvis, which was fixed, and as a result induced a bending moment about the local x-axis measured by the femur load cell.

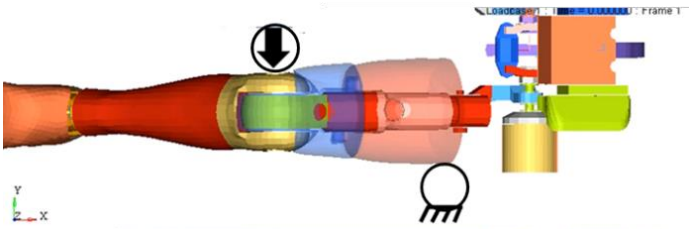

Figure 7. Bending simulation setup with a force acting laterally on the medial aspect of the knee and a constraint on the lateral thigh.

RESULTS AND DISCUSSION

Vehicle Test CAE Model

The occupant kinematics in the CAE model were compared visually in an oblique view from 0 to 60ms at 20ms increments (See Figure 8). The SID-IIs and HBM showed similar kinematic behavior throughout the event.

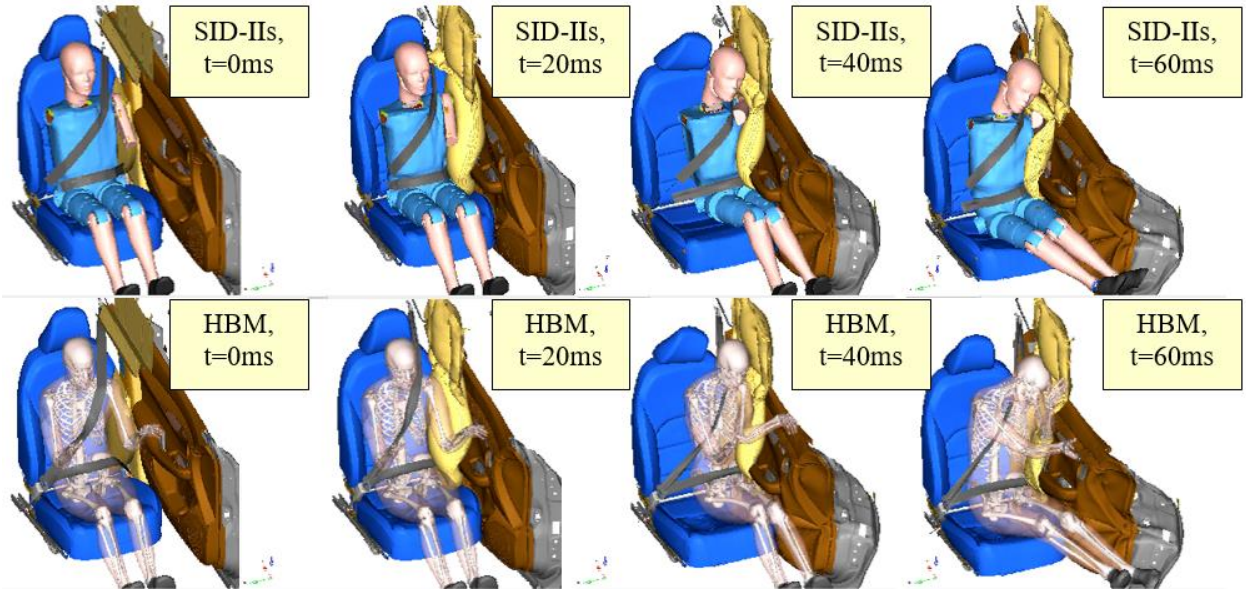

Figure 8. CAE model front view and profile view of SID-IIs and HBM from 0 to 60ms at 20ms increments.

Based on a plan view section of the SID-IIs and HBM at 0ms and 40ms, the SID-IIs exhibits clockwise pelvis Z-axis rotation due to the 'M-shaped' door deformation pattern characteristic of the IIHS Side Impact 2.0 test whereas the HBM pelvis is compressed and pushed laterally inboard rather than rotating (See Figure 9).

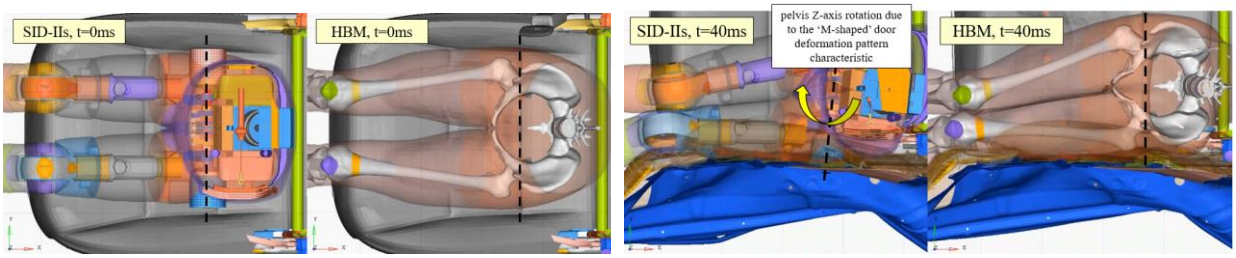

Figure 9. CAE model plan view section of SID-IIs and HBM at 0ms (left) and 40ms (right) showing SID-IIs clockwise pelvis Z-axis rotation.

The HBM injury responses in the CAE model were compared to the SID-IIs and only showed slight variations in loading characteristics and peak values for all body regions except for the HBM's peak femur moment which was seven times less than that of the SID-IIs (See Table 1).

Table 1.
Peak Injury Value Comparison Between SID-IIs and HBM

Injury parameter	**SID-IIs**	**HBM**	**Percent difference**
Head resultant acceleration (g)	50	60	20%
Neck force, Z-axis (N)	1300	1200	8%
Shoulder force, Y-axis (N)	1700	1000	41%
Upper rib deflection (mm)	26	33	27%
Middle rib deflection (mm)	28	27	4%
Lower rib deflection (mm)	32	31	3%
Combined iliac and acetabulum force (N)	6000	5700	5%
Femur moment, X-axis (Nm)	325	44	86%

The loading characteristic of the resultant head acceleration and upper neck force (Z-axis) for the SID-IIs and HBM were similar (see Figures 10 and 11). The peak head resultant acceleration for the SID-IIs was 10g's less compared to the HBM. The peak upper neck force for the SID-IIs was 100N more compared to the HBM. The 10ms earlier ramp up timing observed in the SID-IIs head resultant acceleration and upper neck force (Z-axis) around 20-25ms was attributed to shoulder geometry and stiffness differences between occupants that produce different shoulder loading characteristics (See Figure 12). The SID-IIs shoulder force exhibits the same earlier loading time compared to the HBM, albeit at an earlier event time around 10ms and therefore indicative that the shoulder loading time difference causes the earlier head and neck loading in the SID-IIs. The peak shoulder force for the SID-IIs was 700N more compared to the HBM.

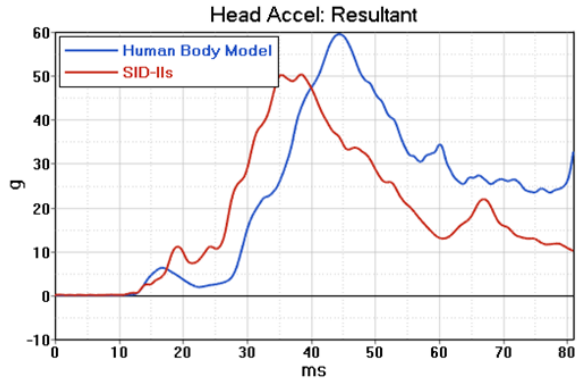

Figure 10. Head resultant acceleration vs. time.

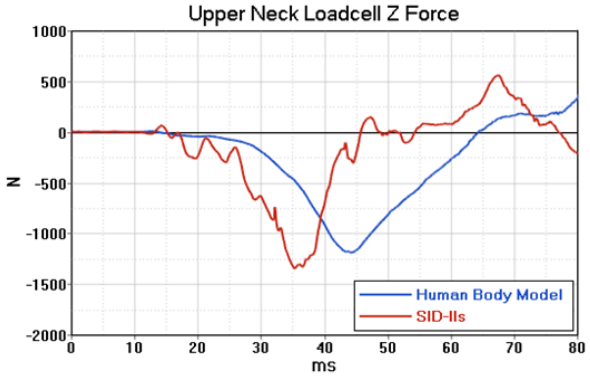

Figure 11. Upper neck force (Z-axis) vs. time.

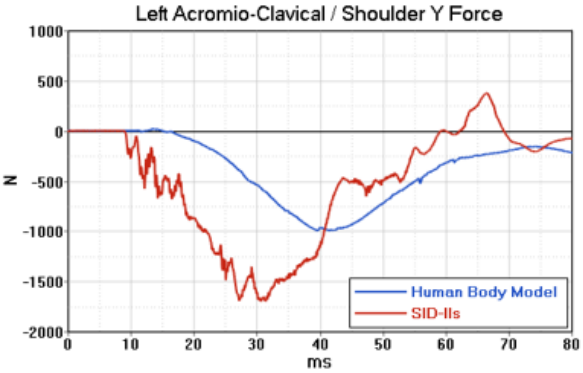

Figure 12. Shoulder force (Y-axis) vs. time.

The loading characteristics and peak values of the upper, middle, and lower thorax rib deflections for the SID-IIs and HBM were similar (See Figures 13, 14, and 15). The peak upper thorax rib deflection was 7mm less in the SID-

IIs compared to the HBM. The SID-IIs middle and lower thorax rib deflections had a longer load duration compared to the HBM but the peak values were approximately the same. The load timing for all thorax rib deflections was well aligned between occupants.

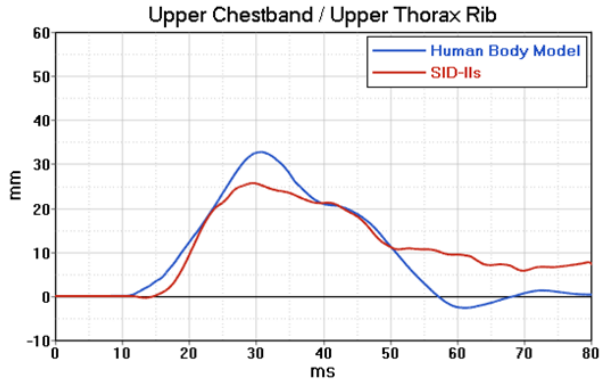

Figure 13. Upper thorax rib deflection vs. time.

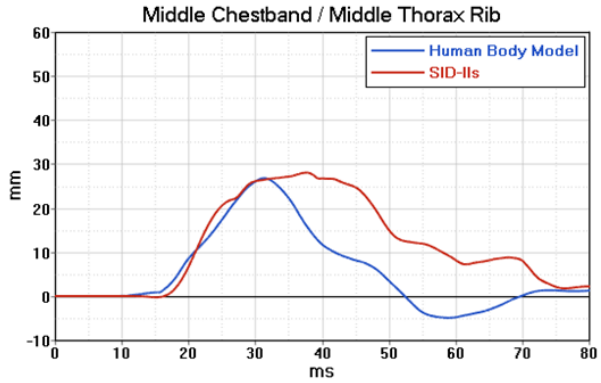

Figure 14. Middle thorax rib deflection vs. time.

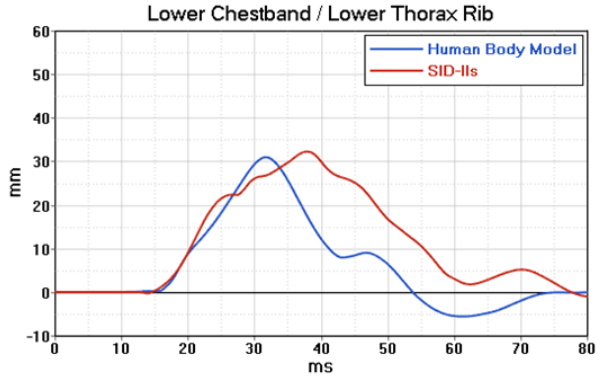

Figure 15. Lower thorax rib deflection vs. time.

The iliac force and acetabulum peak force distribution for the SID-IIs and HBM were not aligned due to differences in occupant geometry (See Figures 16 and 17). However, the loading characteristic and peak value of the combined iliac and acetabulum force (Y-axis) were similar (See Figure 18). The similarity in the combined iliac and acetabulum force indicates that the SID-IIs clockwise pelvis Z-axis rotation caused by the 'M-shaped' door deformation pattern characteristic does not influence pelvis injury performance when compared to the HBM.

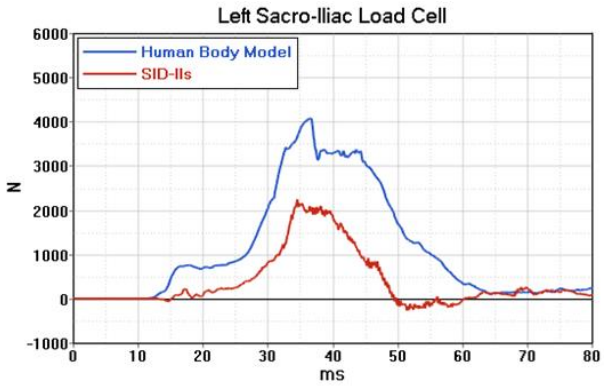

Figure 16. Iliac force (Y-axis) vs. time.

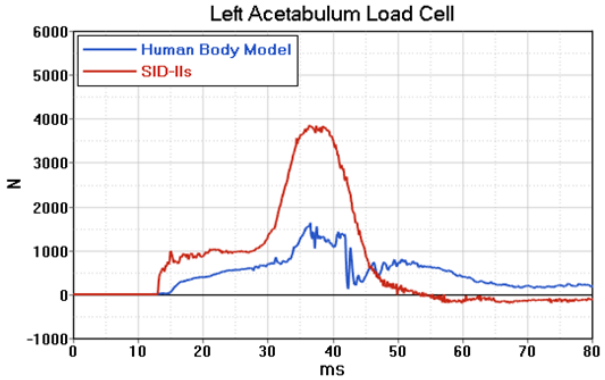

Figure 17. Acetabulum force (Y-axis) vs. time.

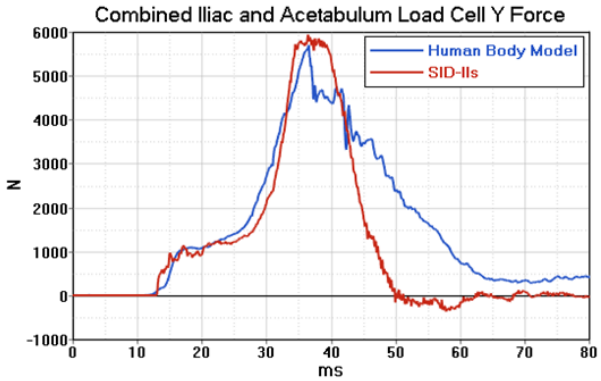

Figure 18. Combined iliac and acetabulum force (Y-axis) vs. time.

The measured SID-IIs femur moment was significantly higher compared to the HBM (See Figure 19). Whereas the HBM experiences minimal femur moment, the peak femur moment in the SID-IIs is nearly seven times higher than the HBM.

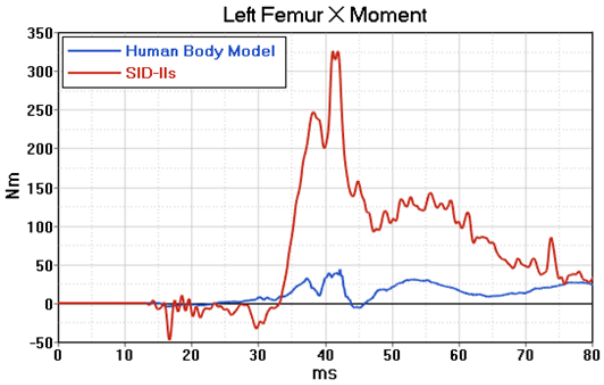

Figure 19. Femur moment (X-axis) vs. time.

There was a femoral neck fracture seen in the HBM simulation results. However, the model was rerun with bone fracture turned off and it was confirmed that the potential loss of load resulting from the femoral neck fracture did not explain the lower femur moment.

Out of all the injury parameters compared between the SID-IIs and the HBM, the femur moment was by far the biggest difference. To further investigate the mechanism causing the difference in peak femur moment, a simplified femur bending test CAE model was created, as discussed previously.

Simplified Femur Bending Test CAE Model

The simplified bending test CAE model was run for both the SID-IIs and HBM occupants. The femur moment was measured as knee displacement was increased from 0 to 100mm (See Figure 20). At approximately 80mm of knee displacement, the SID-IIs femur moment suddenly transitioned from increasing linearly to increasing exponentially between 80 to 100mm of knee displacement. By comparison, the HBM femur moment increases linearly throughout the entire range of knee displacement. During the linear phase of loading, it was observed that the SID-IIs femur moment is almost exactly double the HBM femur moment throughout thigh rotation up until approximately 80mm of knee displacement due to differences in flesh stiffness between the SID-IIs and HBM. This is further indication that a similar loading generates nearly twice the moment in the SID-IIs as compared to the HBM, even at relatively small angles between the femur and pelvis. At larger angles, the difference becomes more extreme due to the biofidelic limitations of the SID-IIs hip ball-joint.

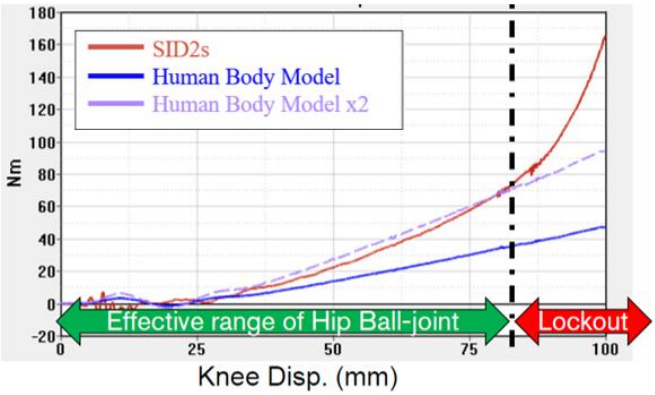

Figure 20. Left femur moment (X-axis) vs. knee displacement for SID-IIs and HBM in bending test CAE model.

After further inspection of a physical SID-IIs dummy, it was found that this CAE model identified the difference in effective range of hip ball-joint between the SID-IIs and HBM. By design, the SID-IIs hip allows for 10-12 degrees of articulation before mechanical joint lockout occurs (See Figure 21). The HBM does not share this design limitation. The limited articulation range for the SID-IIs hip corresponds to a fixed amount of outboard knee displacement in the simplified bending test CAE model, after which the SID-IIs femur moment unrealistically increases exponentially compared to the HBM due to joint lockout.

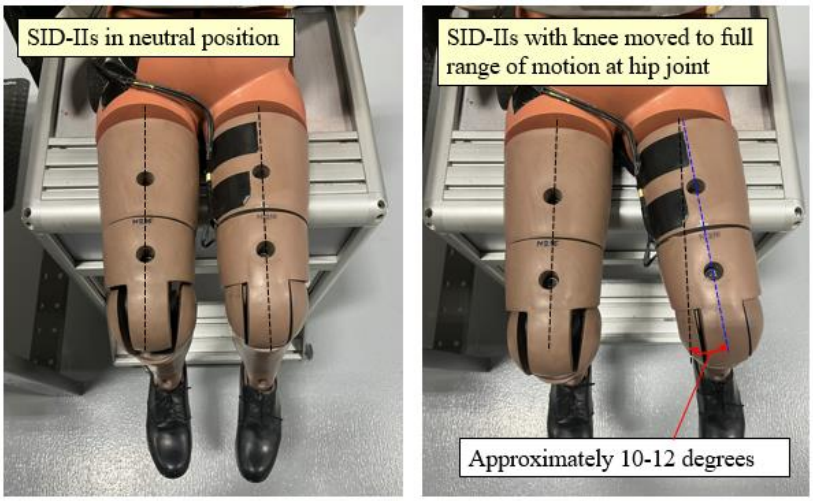

Figure 21. SID-IIs with legs in neutral position compared to SID-IIs with left knee moved to full range of motion at hip joint.

This component test is representative of the SID-IIs clockwise pelvis rotation that occurs in the IIHS Side Impact 2.0 test due to the 'M-shaped' door deformation pattern characteristic. Based on this result, it can be concluded that the limitation of SID-IIs femur biofidelity as currently designed is the root cause for the increased SID-IIs femur moment compared to that of the HBM in the IIHS Side Impact 2.0 test.

CONCLUSIONS

This study analyzed the differences in kinematics and injury responses between the SID-IIs and HBM in the IIHS Side Impact 2.0 test. The occupants had similar kinematics except for the SID-IIs demonstrating clockwise pelvis Z-axis rotation due to the vehicle's M-shaped body deformation pattern characteristic. While the combined iliac and acetabulum force injury response was similar between the occupants, the SID-IIs predicted a significantly higher femur moment due to biofidelic limitations of the hip joint that caused the femur moment to increase exponentially after joint lockout. Therefore, the SID-IIs as currently designed does not provide a biofidelic response for femur moment and pelvis rotation in the IIHS Side Impact 2.0 test when compared to the HBM.

ACKNOWLEDGMENTS

The authors would like to thank Christina Morris, Autoliv, and Pete Luepke, Nissan North America, for their support of this study.

REFERENCES

[1] Dakin, G. J., Arbelaez, R. A., Nolan, J. M., Zuby, D. S., & Lund, A. K. (2003, May). Insurance institute for highway safety side impact crashworthiness evaluation program: impact configuration and rationale. In *18th ESV Conference, Nagoya*.

[2] Arbelaez, R.A., Baker, B.C., and Nolan, J.M., "Delta Vs for IIHS Side Impact Crash Tests and Their Relationship to Real-World Crash Severity", 2005, Proceedings of the 19th International Technical Conference on the Enhanced Safety of Vehicles, Paper Number 05-0049

[3] Brumbelow, M.L., Mueller, B.C., and Arbelaez, R.A., "Occurrence of Serious Injury in Real-World Side Impacts of Vehicles with Good Side-Impact Protection Ratings", 2015, Traffic Injury Prevention, DOI:10.1080/15389588.2015.1020112

[4] Brumbelow, M.L., Mueller, B., Arbelaez, R.A., and Kuehn, M., "Investigating Potential Changes to the IIHS Side Impact Crashworthiness Evaluation Program", 2017, Proceedings of the 25th International Technical Conference on the Enhanced Safety of Vehicles, Paper Number 17-0083

[5] Arbelaez, R.A., Mueller, B.C., Brumbelow, M.L., and Teoh, E.R., "Next Steps for the IIHS Side Crashworthiness Evaluation Program", 2018, 62nd Stapp Car Crash Conference, SC18-02

[6] Mueller, B.C., Arbelaez, R.A., Brumbelow, M.L., Nolan, J.M., "Comparison of Higher Severity Side Impact Tests of IIHS-Good-Rated Vehicles Struck by LTVs and a Modified IIHS Barrier with the Current IIHS Side Test and Real-World Crashes", 2019, Proceedings of the 26th International Technical Conference on the Enhanced Safety of Vehicles, Paper Number 19-0193
[7] Mueller, B., "IIHS Side Impact 2.0 Barrier Development", April 2020, iihs.org
[8] Side Impact Crashworthiness Evaluation 2.0 Ratings Guidelines, September 2021, iihs.org
[9] Irwin, A. L., Mertz, H. J., Elhagediab, A. M., & Moss, S. (2002). Guidelines for assessing the biofidelity of side impact dummies of various sizes and ages. *Stapp Car Crash Journal*, *46*, 297-319.
[10] Rhule, H. H., Maltese, M. R., Donnelly, B. R., Eppinger, R. H., Brunner, J. K., & Bolte, J. H. (2002). *Development of a new biofidelity ranking system for anthropomorphic test devices* (No. 2002-22-0024). SAE Technical Paper.
[11] Yoganandan, N., Pintar, F., Maltese, M., Eppinger, R., Rhule, H., & Donnelly, B. (2002). Biofidelity evaluation of recent side impact dummies. *Proceedings of the IRCOBI, Munich, Germany*, 57-69.
[12] Kemper, A., Stitzel, J., Duma, S., Matsuoka, F., & Masuda, M. (2005, June). Biofidelity of the SID-IIs and a modified SID-IIs upper extremity: biomechanical properties of the human humerus. In *Proc. of the 19th Int. Tec. Conf. on the Enhanced Safety of Vehicles* (No. 05-0123).
[13] Wang, Z. J., Lee, E., Bolte IV, J., Below, J., Loeber, B., Ramachandra, R., ... & Guck, D. (2018). Biofidelity Evaluation of THOR 5th Percentile Female ATD. In *Ircobi Conference, Athens/Greece*.
[14] Kuppa, S., Eppinger, R. H., Mckoy, F., Nguyen, T., Pintar, F. A., and Yoganandan, N. 2003. "Development of side impact thoracic injury criteria and their application to the modified ES-2 dummy with rib extensions (ES-2re)." SAE Technical Paper, No. 2003-22-0010
[15] Perez-Rapela, D., Donlon, J.P., Forman, J.L., Crandall, J.R., Pipkorn, B., Shurtz, B.K., and Markusic, C. 2019. "PMHS and WorldSID Kinematic and Injury Response in Far-Side Events in a Vehicle-Based Test Environment." Stapp Car Crash Journal, No. 63, 83-126

APPENDIX

Table A.
A Summary of the Common Injury Parameters Between IIHS Side Impact 1.0 and 2.0 Test and their Associated Injury Protection Ratings

			IIHS Side Impact 1.0			IIHS Side Impact 2.0		
Body Region	**Parameter**	**IARV**	**Good/Acceptable**	**Acceptable/Marginal**	**Marginal/Poor**	**Good/Acceptable**	**Acceptable/Marginal**	**Marginal/Poor**
Head and Neck	Head Injury Criterion (HIC) 15	779	623	779	935	623	779	935
	Neck Axial Tension (kN)	2.1	2.1	2.5	2.9	2.1	2.5	2.9
	Neck Compression (kN)	2.5	2.5	3.0	3.5	2.5	3.0	3.5
Torso	Average Rib Deflection (mm)	34	34	42	50	28	38	48
	Worst Rib Deflection (mm)	N/A	*	*	*	*	*	*
	Rib Deflection Rate (m/s)	8.20	8.20	9.84	11.48	8.2	9.8	11.5
	Viscous Criterion (m/s)	1.00	1.00	1.20	1.40	1.0	1.2	1.4
Pelvis	Combined Acetabulum and Ilium Force (kN)	5.1	5.1	6.1	7.1	4.0	5.0	6.0